Probing Lung Microstructure with Gradient Echo Plural Contrast Imaging

Alexander L Sukstanskii[1], James D Quirk[1], and Dmitriy A Yablonskiy[1]
[1]*Radiology, Washington University, St. Louis, Missouri, United States*

Introduction The in vivo lung morphometry technique, relying on measuring Brownian motion of inhaled hyperpolarized gas in lung airspaces, makes it possible to obtain in vivo information on lung microstructure at the alveolar level [1-3]. This communication presents a theoretical background and experimental method for a new approach to study lung microstructure, that is based on $T2^*$-relaxation properties of hyperpolarized gas in lung airspaces. $T2^*$ relaxation depends on tissue-specific mesoscopic magnetic field inhomogeneities induced by the susceptibility differences between lung tissue (alveolar septa, blood vessels) and lung airspaces. Based on Monte-Carlo computer simulations of diffusion of ^{3}He atoms in the acinar airway tree, we derive analytical expressions relating the time-dependent MR signal to the geometrical parameters of acinar airways and blood vessel network and test our theory on healthy volunteers using in vivo data obtained with a multi-gradient echo sequence.

Theory The MR signal time dependence can be presented in the form $S(t) = S_0 \cdot \exp(-\Gamma(t)) \cdot F(t)$, where $F(t)$ describes the effects of signal decay due to the macroscopic field inhomogeneities (4), whereas the attenuation function $\Gamma(t) = \Gamma_s(t) + \Gamma_b(t)$ describes relaxation of hyperpolarized gas in the lung airspaces due to the mesoscopic magnetic field inhomogeneities induced by the susceptibility difference $\Delta\chi$ between lung airspaces and surrounding tissue - alveolar septa, $\Gamma_s(t)$, and blood vessels, $\Gamma_b(t)$. The contribution of the blood vessels can be described in the framework developed in (5): $\Gamma_b(t) = R2^* \cdot t$, where $R2^* = 4\pi/3 \cdot \gamma \cdot \Delta\chi \cdot B_0 \cdot \zeta$ (ζ is the mid-size blood vessel volume fraction, B_0 is the external field and γ is the gyromagnetic ratio). To analyze the contribution of alveolar septa, we performed Monte-Carlo simulations using the Weibel model of acinar airways [6] adopted in [1-3]. In this model, an acinar airway is considered as a cylinder of radius R covered by a sleeve of alveoli of depth h. Analytical expressions for the magnetic field induced by the alveolar septa of effective thickness d within a single airway are found in [3]. A typical experimentally found value of $T2^*$ is about several tens of milliseconds [7-11]. In this time range, ^{3}He atoms can diffuse over distances much longer than the average length of individual airways (~ 1 mm), and the branching structure of acinar airway tree should, therefore, be taken into account. In our simulations, we use a model comprising 9 generations of branches corresponding to the 9 generations of acinar airways in human lungs. The simulations have been performed with $\Delta\chi = 0.72\,\text{ppm}$, $B_0 = 1.5\,\text{T}$ and the broad range of the model geometrical parameters: $R = 300-400\,\mu\text{m}$, $h/R = 0.2-0.5$, $d = 10-25\,\mu\text{m}$. The signal attenuation strongly depends on the input parameters. However, a close inspection of the results reveals an amazing scaling relationship: in the interval $t < 30\,\text{ms}$, all the curves corresponding to different input parameters can be well described by the universal expression $\Gamma_s(t) = (\delta\omega \cdot t)^2/2 \cdot \Phi\left(t/t_D\right)$, where $\delta\omega$ is the dispersion of the Larmor frequency distribution, dependent on the geometrical parameters of the model, $t_D = R^2/D_L$ is the characteristic diffusion time, $D_L = D_0 \cdot \exp\left[-2.89 \cdot (h/R)^{1.78}\right]$ is the longitudinal diffusion coefficient depending on R and h (1), D_0 is the free diffusion coefficient. The universal function $\Phi\left(t/t_D\right)$ (for 75 different sets of the input parameters) is shown in Figure 1.

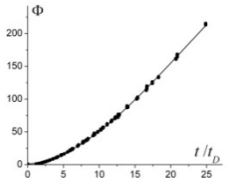

Methods The data were obtained from 8 subjects (age 26 ± 7, never-smokers) who provided informed consent and procedures were performed with approval from the FDA and local IRB. ^{3}He gas was hyperpolarized using a Nycomed Amersham Imaging IGI.9600.He polarizer. The data were acquired using a 3D multi-gradient-echo sequence with 7x7x10 mm^3 resolution (flip angle θ=3.5°, TR=22 ms, 10 gradient echoes, TE_1=2ms and echo spacing ΔTE=2 ms).

Results The model described above makes it possible to extract the parameters $\delta\omega$, t_D and ζ from the experimentally measured data. Figure 2 shows examples of ζ (upper panel) and t_D (ms, lower panel) maps. The map of t_D is rather homogeneous, and its average value, $t_D = 2.1 \pm 0.13\,\text{ms}$ (mean ± std over all the subjects), is in a good agreement with that calculated from multi-b diffusion independent measurements for the same subjects: $R = 311 \pm 7\,\mu\text{m}$, $h = 145 \pm 14\,\mu\text{m}$, $t_D = 2.5 \pm 0.3\,\text{ms}$. High values of ζ in the central lung correspond to areas with high concentrations of large blood vessels. Outside of this area, $\zeta = 4 \pm 0.8\,\%$. The average $\delta\omega = 0.20 \pm 0.02\,\text{ms}$ leads to the effective (apparent) septa thickness $d = 18 \pm 2\,\mu\text{m}$.

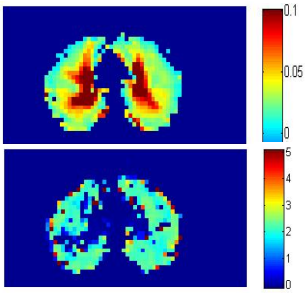

While $T2^*$ measurements of hyperpolarized gas in lungs were reported previously [7-11] and even used for early detection of metastatic cancer cells in the lungs [10], a theory of $T2^*$- relaxation was not previously developed. Importantly, our model predicts substantially non-monoexponential signal behavior and fits experimental data in most regions of the lungs (except large vessels).

Conclusion A new approach – Gradient Echo Plural Contrast Imaging (GEPCI) of lungs – is proposed for simultaneously extracting information about lung ventilation, acinar airways geometric parameters and blood vessel network structure from a single multi-gradient echo experiment. Measurements obtained in 8 healthy volunteers are in good agreement with literature values.

This study is supported by NIH R01HL70037.

1. Yablonskiy et al, JAP 2009; 107: 1258. 2. Sukstanskii et al, JMR 2010; 207:234. 3. Yablonskiy et al, MRM 2013 (review). 4. Yablonskiy et al, MRM 2013; 70: 1283. 5. Yablonskiy and, Haacke, MRM 1994; 32:749-763. 6. Weibel ER, Morphometry of the human lung. Berlin: Springer-Verlag, 1963. 7. Bock, MRM 1997; 38:890. 8. Chen, et al, MRM 1999, 42: 729. 9. Salerno, et al, MRM 2005; 53:212. 10. Deppe, et al, JMRI 2009; 30:418. 11. Branca, et al, PNAS 2010; 107:3693.